A high-throughput screening assay based on TR-FRET to identify inhibitors for *T. brucei* kinases

Zeba Islam

A thesis

submitted in partial fulfillment of the

requirements for the degree of

Master of Science

University of Washington

2018

Committee:

Dustin J Maly

Robert E. Synovec

Program Authorized to Offer Degree:

Department of Chemistry

University of Washington

Abstract

A high-throughput screening assay based on TR-FRET to identify inhibitors for *T. brucei* kinases

Zeba Islam

Chair of the Supervisory Committee:

Dustin J. Maly

Department of Chemistry

African Sleeping Sickness or Human African Trypanosomiasis (HAT) is one of the most under studied tropical diseases and continues to be a threat to more than 65 million people in sub-Saharan Africa. It is caused by the bite of a tsetse fly infected with a trypanosome known as *Trypanosoma brucei*. Therapeutic advances have been made in combating the disease, but a high mortality rate of 5%, and the unavailability of treatments for later stages, begets a need for more effective therapeutics. Because kinases are attractive drug targets, we explored the druggability of three *Trypanosoma brucei* kinases that have been demonstrated to be essential for the survival of the trypanosome, and thus potential drug targets for HAT. Here, we describe a TR-FRET-based assay for the three kinases to identify and confirm inhibitor hits from a kinase inhibitor library of 429 compounds. In our screen, we identified inhibitors belonging to

the *type II* class of kinase inhibitors, with low nanomolar potency (IC_{50}) against several of these three essential kinases. These inhibitors provide new hits for lead optimization with the aim of identifying new drug treatments for HAT.

Acknowledgments

I would like to thank my parents for their eternal and unconditional love, help and support at every stage of my life, that has truly helped me face challenges and become the person I am today. I would like to thank my elder brother for all the laughter and mentoring that has helped me learn to take life with a pinch of salt. I dedicate my work to my father, who has been a role model to me, and has always had my best interests in mind. Their good wishes from miles away has been a driving factor to strive each day.

I would also like to thank my co-workers and friends from the Maly lab for all the fun and support. It has been a wonderful learning experience. I would like to thank Linglan and Gayani for their positivity and guidance, and Sujata, for being a caring friend and mentor, and being extremely patient with me from my early research days.

I would like to thank my adviser, Dustin Maly for his guidance and support. His continued efforts have helped me develop a scientific edge and think about broader perspectives that I believe will be of great value to me in my future.

My journey in UW would have been incomplete without my friends from school and undergraduate years. Their constant care and love for years, has always given me a sense of stability and strength. I would like to thank my Seattle family, particularly Manan, Krishna and Prabhleen for their guidance and affection. I would like to thank Pravesh for being a constant emotional support and bringing positivity to my life in the past year, that has helped me stay happy and focused in the most difficult times. This work would not have been possible without him and I am indebted to him for it.

Lastly, and most importantly, I would like to thank Prof. Synovec and the Department of Chemistry at UW for their support.

TABLE OF CONTENT

List of Figures ……..... i

List of Tables ……..... ii

Appendix & Supplementary Information……..…..... iii

List of Abbreviations ……..... iv

Introduction ……..... 1

Materials and Methods ……..... 5

Results and Discussions ……..... 9

Conclusion …….. 22

References ……... 23

Appendix..... 25

List of Figures

Figure 1. Schematic of LANCE TR-FRET assay.

Figure 2. (A) Binding assay data for Tb11.46.0003 at various kinase and SCP2 probe concentrations. (B) Binding assay data for Tb927.4.5310 at various kinase and SCP2 probe concentrations. (C) Binding assay data for Tb927.3.2440 at various kinase and SCP2 probe concentrations.

Figure 3. Structure of inhibitor GP29 used in assay against Tb11.46.0003 & Tb927.4.5310.

Figure 4. (A) Heatmap showing screening results for Tb11.46.0003. (B) Heatmap showing screening results for Tb927.4.5310. (C) Heatmap showing screening results for Tb927.3.2440. Color gradient for % inhibition shown alongside.

Figure 5. Dose-response curves for Rebastinib, SC1 (Pluripotin), RAF-265 & GZD824 against Tb11.46.0003 & Tb927.4.5310.

Figure 6. Binding curves for SCP2 probe against Tb11.46.0003 (80 nM) & Tb927.4.5310 (80 nM).

List of Tables

Table 1. Summary of FRET ratios of reaction mixture comprising of inhibitor with SCP2 probe and kinase, positive control and negative control against Tb11.46.0003, Tb927.4.5310 & Tb927.3.2440.

Table 2. List of hits from kinase inhibitor library screening of Tb11.46.0003.

Table 3. List of hits from kinase inhibitor library screening of Tb927.4.5310.

Table 4. Summary of IC_{50} and K_i values for the 4 inhibitors RAF-265, Pluripotin, Rebastinib and GZD824 against Tb11.46.0003 & Tb927.4.5310.

Table 5. List of hits from kinase inhibitor library screening of Tb927.3.2440 (AEK1).

Appendix

Table A1. FRET ratio of multi-well reaction mixtures comprising of inhibitor GP29, positive control and negative control for Tb11.46.0003 (concentrations mentioned in brackets).

Table A2. FRET ratio of multi-well reaction mixtures comprising of inhibitor GP29, positive control and negative control for Tb927.4.5310 (concentrations mentioned in brackets).

Table A3. FRET ratio of multi-well reaction mixtures comprising of inhibitor VI-27, positive control and negative control for Tb927.3.2440/AEK1 (concentrations mentioned in brackets).

Figure A1. (A) Structure of RAF-265. (B) Structure of GZD824. (C) Structure of SC1 (Pluripotin). (D) Structure of Rebastinib.

Supplementary Information

Table S1. Heatmap setup with name of inhibitors

List of Abbreviations

AEK1	AGC essential kinase 1
BODIPY	Boron-dipyrromethene
BSA	Bovine Serum Albumin
Cy	Cyanine
DCM	Dichloromethane
DIPEA	N, N-Diisopropylethylamine
DMSO	Dimethyl sulfoxide
EDC	N-(3-Dimethylaminopropyl)-N′-ethylcarbodiimide hydrochloride
Eu	Europium
FRET	Fluorescence energy transfer
HAT	Human African typanosomiasis
HCl	Hydrochloric acid
His	Histidine
HTS	High throughput screening
LANCE	Lanthanide chelate excite
mg	Milligrams
mL	Milliliter
mM	Millimolar
nm	Nanometer
nM	Nanomolar
N	Normal
NaCl	Sodium Chloride
rpm	Rotations per minute

NaOH	Sodium Hydroxide
Na_2SO_4	Sodium sulfate
TFA	Trifluoroacetic acid
TR-FRET	Time resolved fluorescence energy transfer
μM	Micromolar
μL	Microliter

Introduction

Human African trypanosomiasis (HAT), also known as African sleeping sickness is a threat to more than 65 million people in 36 sub-Saharan Africa countries. It is one of the major neglected tropical diseases that has led to multiple epidemic breakouts in the past century [1]. HAT is caused by the protozoan parasite *Trypanosoma brucei: T. b. rhodesiense* and *T. b. gambiense* in East and West Africa respectively, transmitted by the bite of the tsetse fly (genus *Glossina*) [2, 3]. When an infected tsetse fly bites a human, the first symptoms are noticed within 5 days. At this point, the trypanosomes have entered and spread in the bloodstream, lymph nodes, and other systemic and endocrine organs. This is the haemolymphatic stage (stage 1), with non-specific, regular symptoms like intermittent fever, painless skin chancre, headaches, lymphadenopathy, muscle and joint pains, etc. For this reason, HAT is often undiagnosed at early stages. Once the trypanosomes cross the blood-brain barrier, they enter the central nervous system leading to meningoencephalitis. This is the late, encephalitic stage (stage 2), with severe symptoms like daytime somnolence, nighttime insomnia, reduced neurological functions, like behavioral changes, partial paralysis, progressive confusion, etc. If untreated, it can be fatal, and may lead to coma or ultimately death [4, 5, 6, 7, 8].

While progress has been made in finding more effective diagnostic tools and therapeutic drugs for HAT, it is still a critical issue in hand due to insufficient knowledge of the clinical and mechanistic features of the infection [9]. Currently, there are 4 registered drugs for the treatment of HAT, administered based on the stage and infecting trypanosome. Since 2009, a combination of eflornithine and nifurtimox (NECT) has been used for the treatment of gambiense human African trypanosomiasis (stage 2), while there is still no treatment for rhodesiense human African trypanosomiasis (stage 2) [10]. Although the number of reported

cases has declined drastically in the past decade, toxicity (mortality rate of 5%), potential for developing drug resistance, chances of relapse, and lack of vaccination due to the parasite's ability to evade host immune response, makes it imperative to find more effective therapeutic drugs to eliminate HAT [11].

Kinases as drug targets

Kinases are one of the largest family of enzymes that regulate vital cell signaling pathways by catalyzing the transfer of γ-phosphate of ATP onto a substrate protein. Thus, in several diseases, perturbation of cell functions is linked to deregulation of kinase mediated signal transduction, making kinases a popular drug target [12].

While kinases manage diverse functions in cells, key amino acid residues in its catalytic core are highly conserved. The ATP binding core of kinases lies in between its small N-terminal and larger C-terminal lobe. A conserved lysine residue in the β3 sheet of the N-lobe forms a salt bridge with a conserved glutamate residue in the αC-helix within the same lobe. This is essential for the kinase to be active and is associated with a conformation in which the αC-helix is in an 'in' position. In the catalytic core around the site of phoshphoryl transfer, a conserved DFG motif is also essential for its catalytic activity and is associated with an active conformation in which it is in the DFG- 'in' position. *Type I* inhibitors are a class of ATP competitive inhibitors that bind to the kinase in its active conformation with both αC-helix and the DFG motif in an 'in' position, whereas the *type II* class of ATP-competitive inhibitors bind to the kinase in the inactive DFG - 'out' conformation. The *type II* inhibitors target non-conserved hydrophobic pockets near the ATP-binding core, created by the movement of the DFG motif, making them highly potent and selective drugs for various diseases. This has made this class of inhibitors an active field of research for identifying drugs for kinases that are misregulated in many diseases [13 ,14, 15].

The *T. brucei* protein kinome includes 170 protein kinases, and a genome wide RNAi screen recognized more than 40 essential kinases, that could serve as potential drug targets for HAT [16]. Previous studies in our lab identified 2 of these essential kinases – NEK family kinase Tb 927.4.5310 and STE family kinase Tb 11.46.0003 that have a strong affinity for a *type II* inhibitor GP29, using chemical proteomics and RNAi-knockout experiments. Another essential AGC family kinase Tb 927.3.2440 (AEK1), has also shown strong prospects of being a drug target for sleeping sickness, using genetic and chemical validation tools [17]. Following target validation of these 3 kinases, the primary focus of this study was to detect lead small molecules and pharmacophores for future drug discovery of HAT, and possibly, detailed mechanistic studies of the same.

High-throughput screening assay to identify inhibitor hits

To recognize potential hit compounds for a drug target, the most common approach has been to use a high throughput screening technique using a diverse library of inhibitors and screening it against the protein of interest. Screening protocols can vary largely, from *in vitro* biochemical assays like activity assays or binding assays, to cell based-assays. For the assays to be used in high throughput techniques, they must be fast, robust, reproducible, sensitive, and quantitative. *In vitro* biochemical assays are mostly based on fluorescence, bioluminescence or radioactivity. In activity assays, compounds with high inhibitor activity are recognized by monitoring the inhibition of phosphorylation of a substrate by an active target protein, while in binding assays, compounds with high binding affinity are identified by competing against a binding substrate to the target protein. Binding assays are advantageous as they do not require active recombinant proteins to recognize hits and are a good approximation of the inhibitory activity of ATP competitive inhibitors that bind to the active sites of kinases, if not a direct readout like in activity assays [18, 19].

Assay Development

Time resolved fluorescence energy transfer (TR-FRET) is a well-established HTS amenable assay technique, that is used extensively for generating hits for a target protein. The time delayed measurement of fluorescence from the acceptor fluorophore reduces the background fluorescence, as well as interfering fluorescence signal from the inhibitor library compounds [20]. LANCE (Lanthanide chelate excite) TR-FRET assay technology is a sensitive, and homogeneous (no wash) technique for drug discovery screening. The donor fluorophore is a LANCE Eu chelate, that binds to the N-terminus of a His-6-tagged protein through an antibody, and the acceptor fluorophore is a Cy5 dye coupled to a pan-kinase inhibitor that binds to the protein. When the assay mixture is excited at 340 nm, and the substrate is bound to the protein, bringing the acceptor and donor fluorophores at FRET permissible distance, it results in emission at 665 nm (Figure 1) [21]. This is a robust technique to probe inhibitors that bind to

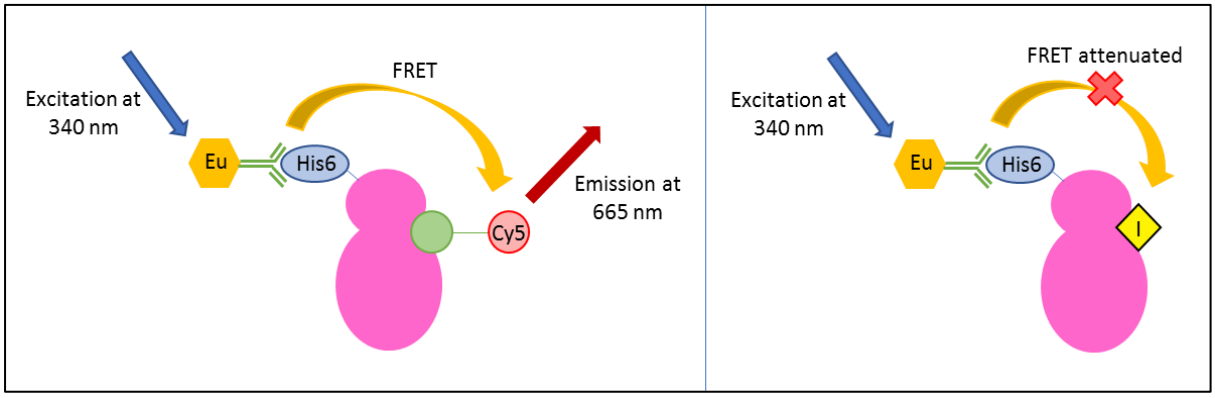

Figure 1. Schematic of LANCE TR-FRET assay.

the protein by competing away the substrate, attenuating FRET. A TR-FRET based assay was developed earlier in our lab to be used for screening inhibitor libraries. An ATP-competitive substrate attached to a Cy5 dye, called SCP2 probe has also been synthesized and optimized to bind to multiple kinases in their active site, including Src and JNK1, yielding high FRET ratios.

Materials & Methods

Protein purification

The recombinant His-6 tagged kinases were cloned into vector AVA0421 and purified in *E. coli* using the protocol followed in this paper [22].

Synthesis of GP29, VI-27 and SCP2

GP29 was synthesized according to the previously published protocol [23].

VI-27 was synthesized by the synthetic route mentioned below.

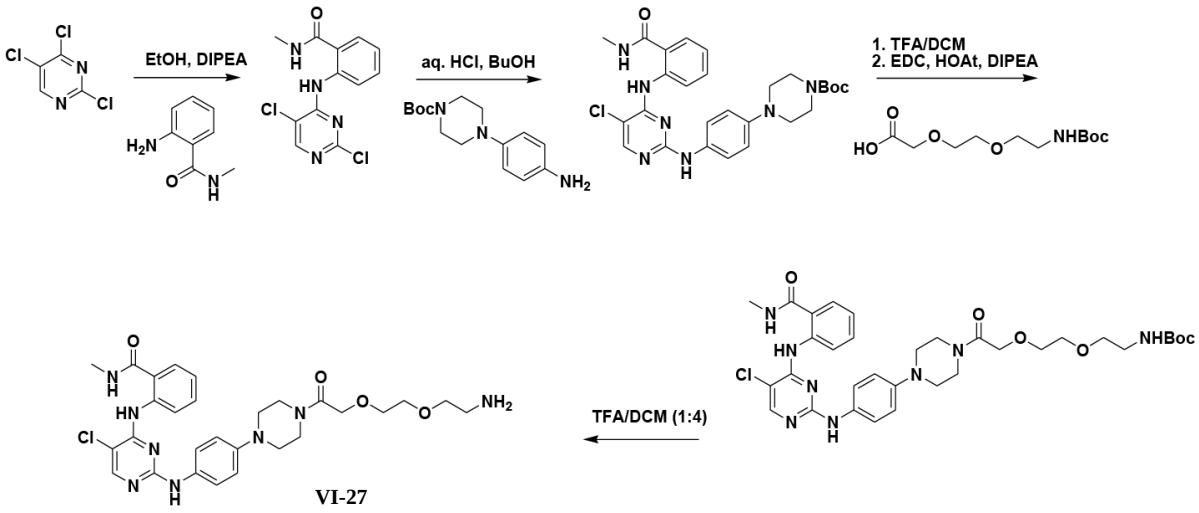

2,4,5-Trichloro pyridine (1 equivalent = 5.45 mmol) and 2-Amino-N-methylbenzamide (1 equivalent) were dissolved in 25 mL of ethanol. DIPEA (2 equivalents) was added to the reaction mixture at room temperature with stirring for 24 hours. The solid was filtered, washed with ethanol and air dried to be used without further purification for the next step. The solid (1 equivalent) and 1-Boc-4-(4-aminophenyl) piperazine (1 equivalent) were added in a microwave vial with a magnetic stir bar, to which 377 µL of 37% HCl was added, and the sealed vial was heated at 100 °C for 24 hours. The solid was filtered off and washed with n-butanol, air dried and used without further purification for the next step. The obtained product

(1 equivalent) was dissolved in 2 mL of DCM and 0.5 mL of TFA was added to it with stirring at room temperature for 2 hours. The reaction mixture was concentrated and the residual TFA was removed by co-evaporating with toluene. The free base of the product of this reaction (1.5 equivalents), 1-Hydroxy-7-azabenzotriazole [HOAt] (1.5 equivalents) and DIPEA (3 equivalents) were added to 1 mL of dry DMF and cooled to 0 °C. To this reaction mixture, N-(3-Dimethylaminopropyl)-N-ethylcarbodiimide hydrochloride [EDC] (1.5 equivalents) was added and stirred overnight at room temperature. The reaction mixture was diluted with 20 mL of ethyl acetate, washed two times with aqueous 1N NaOH solution, followed by water and brine solution. The organic layer was dried over Na_2SO_4, concentrated, and the crude reaction mixture was purified by column chromatography using DCM and 0-10% methanol as a mobile system. The product obtained from this reaction (100 mg) was dissolved in 2 mL of DCM and 0.5 mL of TFA was added to it, with stirring at room temperature for 2 hours. The reaction mixture was concentrated and residual TFA was removed by co-evaporation with toluene. The final product VI-27 was purified by column chromatography using DCM and 0-10% methanol (methanol contains 2% aqueous ammonium hydroxide solution) as a mobile system.

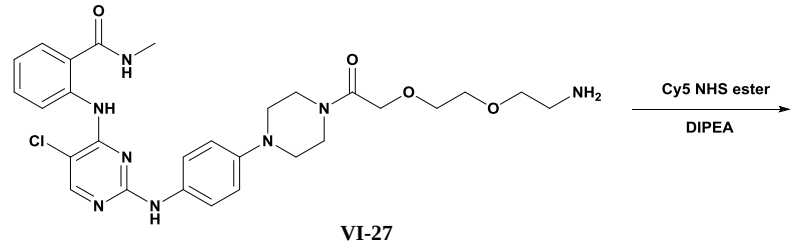

VI-27

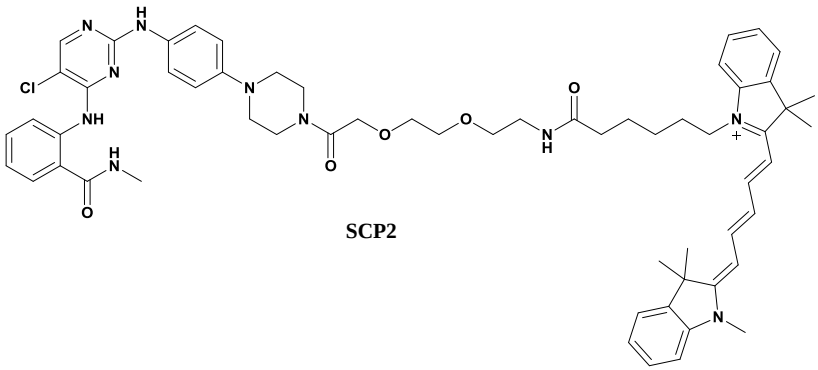

SCP2

VI-27 was coupled to a Cy5 dye to synthesize SCP2 probe. One equivalent of VI-27 was added to one equivalent of Cyanine5 NHS ester (from Lumiprobe) and three equivalents of DIPEA in DMF (1 equivalent = 200 mM). The reaction was left overnight in the dark in an eppendorf tube and was diluted in 50:50 acetonitrile:water. The SCP2 probe was then purified using High Performance Liquid Chromatography, and the structure was confirmed using Mass Spectrometry.

Kinase inhibitor library

The kinase inhibitor library comprising of 429 compounds, was obtained from Selleckchem (pre-dissolved in DMSO, 10 mM) in 96-well format plates (Cat. #L1200). It was diluted in two 384 well Proxi plates (PerkinElmer, MA, USA), to a concentration of 25 μM in DMSO for the primary screen.

The 4 inhibitors used for hit validation, Rebastinib, Pluripotin, GZD824 and RAF-265 were obtained from commercial suppliers and diluted in DMSO to make 20 mM solutions.

TR-FRET assay

The TR-FRET assay was performed using LANCE® time resolved fluorescence assay using the manufacturer's instructions. The inhibitor was diluted in DMSO from its stock solution to 25 times the desired concentration in the assay. The SCP2 probe was diluted from a stock solution of 2.5 mM in DMSO to 100 times the desired concentration in the assay, and further diluted to 6.25 times the desired concentration in the assay buffer (50 mM Tris, 100 mM NaCl, 1 mg/mL BSA at pH 8.0). The no kinase buffer contained only the LANCE Eu-W1024 labeled anti-6XHis antibody (PerkinElmer, MA, USA), and was diluted from a stock concentration of 3.125 μM to 1.25 nM in the assay buffer. The kinase was diluted from its stock solution to 1.25 times the desired concentration in assay buffer containing 1.25 nM antibody. The assay mixture

was made by adding 3.2 µL of the SCP2 probe to 0.8 µL of DMSO/Inhibitor, followed by 16 µL of the kinase/no kinase diluted in assay buffer with the Eu labeled antibody, to a final volume of 20 µL in triplicates in a 384-well Proxi plate (PerkinElmer, MA, USA), and incubated at room temperature for an hour. The plate was spun down at 2000 rpm for 2 minutes at 22 °C prior to fluorescence measurement. The plate was scanned for FRET with an EnVision® Multilabel Reader (PerkinElmer, MA, USA) using a 340 nm excitation filter, and emission filters at 615 nm and 665 nm. The FRET ratio was reported as ratio of the fluorescence signal from the 665 nm channel to that from the 615 nm channel multiplied by a factor of 1000.

Data analysis

The FRET ratio was measured as the ratio of signal count from 665 nm channel to signal count from 615 nm channel, multiplied by a factor of 1000.

The % inhibition of inhibitors was calculated using the average FRET ratio of the assay mixture containing the inhibitor ($FRET_{Inh}$), positive control ($FRET_{PC}$) and negative control ($FRET_{NC}$) used for the experiment as follows:

$$\% \text{ Inhibition} = \% \text{ Binding}_{Inh} = 100*[(FRET_{PC}) - (FRET_{Inh})] / [(FRET_{PC}) - (FRET_{NC})]$$

The % binding of SCP2 probe to the kinase was calculated using the average FRET ratio of the assay mixture containing the SCP2 probe and kinase ($FRET_{SCP2}$) and the assay mixture containing only the SCP2 probe and no kinase ($FRET_{NK}$). The highest FRET ratio signal was calculated from the graph when it reached a plateau ($FRET_{Max}$).

$$\% \text{ Binding}_{SCP2} = 100*[(FRET_{SCP2}) - (FRET_{NK})] / [(FRET_{Max}) - (FRET_{NK})]$$

Results & Discussions

Assay Optimization

I. Optimal concentration of kinase and SCP2 probe

To screen the inhibitor library against the three kinases to identify hits, the conditions for the assay had to be optimized to detect the inhibitor potency. Optimal concentration of the SCP2 probe and kinase had to be determined to yield high enough signal/noise ratio (FRET ratio) that would be attenuated by an inhibitor. For this experiment, different concentrations of SCP2 probe at 400 nM, 800 nM, 1600 nM, 2400 nM and 3200 nM were used for the assays, along with combinations of kinase concentrations at 40 nM, 80 nM, 120 nM, 160 nM, 240 nM and 320 nM. The maximum FRET ratio was calculated for a reaction mixture of DMSO, SCP2 probe at 6.25 times the desired concentration and kinase at 1.25 times the desired concentration (diluted in the assay buffer with 1.25 nM of the antibody). The background FRET ratio was determined using a reaction mixture of DMSO, SCP2 probe at 6.25 times the corresponding concentration and the assay buffer comprising of 1.25 nM of the antibody without any kinase. A combination of the concentration of the SCP2 probe and kinase at which at least a 4-5 fold difference in the FRET ratio was observed in comparison to its background, was selected for the inhibitor library screening.

For the kinase Tb11.46.0003, at lower concentrations of the kinase tested at 40 nM and 80 nM, less than 2.5 fold difference in FRET ratio was observed as compared to the background signal, at even the highest SCP2 probe concentration of 3200 nM (Figure 2 A). Hence the kinase concentration chosen for further experiments was 160 nM, and the SCP2 probe concentration was set at 1.6 μM, at which nearly 4.5 fold difference was observed in the FRET ratio as compared to an average background FRET ratio of 6.83.

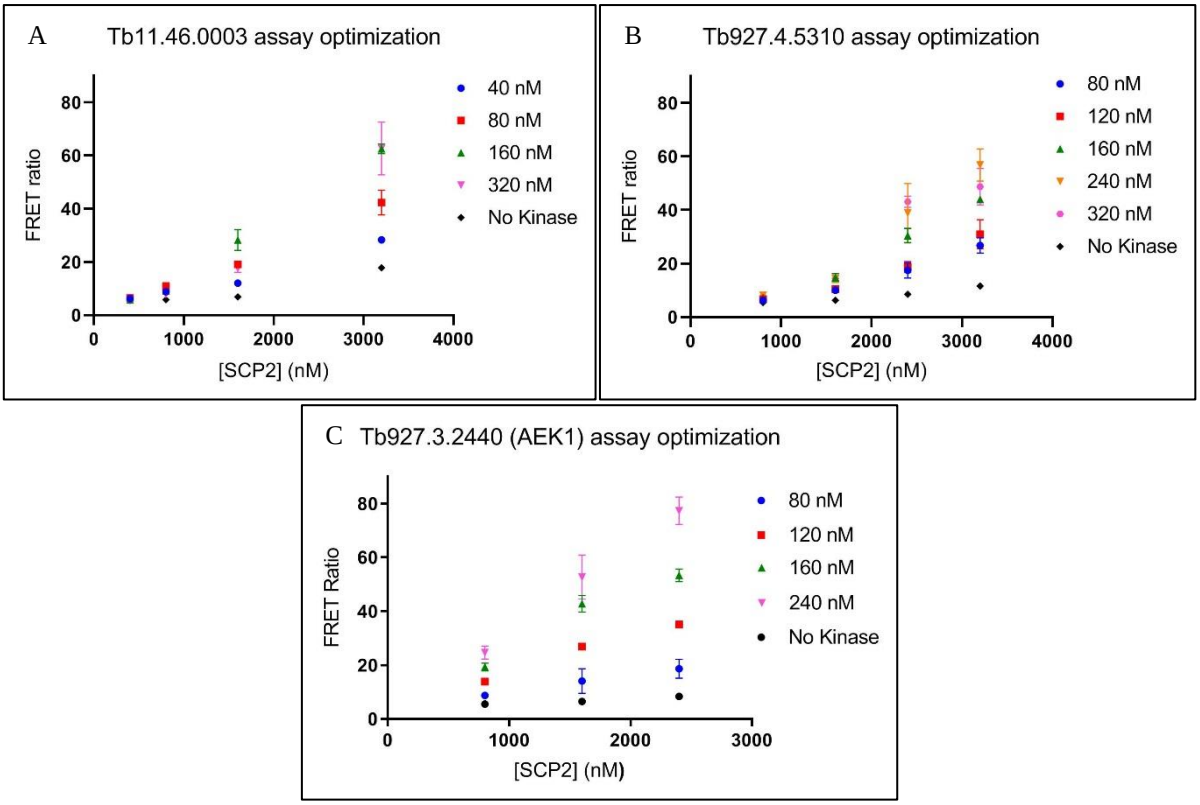

Figure 2. (A) Binding assay data for Tb11.46.0003 at various kinase and SCP2 probe concentrations. (B) Binding assay data for Tb927.4.5310 at various kinase and SCP2 probe concentrations. (C) Binding assay data for Tb927.3.2440 at various kinase and SCP2 probe concentrations.

For the kinase Tb927.4.5310, at lower concentrations of kinase tested at 80 nM and 120 nM, 2.5-3 fold difference in FRET ratio was observed at the highest SCP2 probe concentrations as compared to the background (Figure 2 B). At a higher kinase concentration of 160 nM, nearly 4-fold difference in FRET ratio was observed at a SCP2 probe concentration of 3.2 μM. However, at a kinase concentration of 240 nM and SCP2 probe concentration of 2.4 μM also, the FRET ratio was 4.5 fold higher than the background FRET ratio. These concentrations were preferred for further experiments due to a lower background FRET ratio of 8.55 at a SCP2 probe concentration of 2.4 μM, as compared to 11.6 at higher SCP2 probe concentration of 3.2 μM. For the kinase Tb927.3.2440 (AEK1), at its lowest concentration of 80 nM, a maximum

FRET ratio difference of only ~2.5 fold was observed at the highest SCP2 probe concentration used (2.4 μM) (Figure 2 C). When the protein was used in the reaction mixture at a concentration of 120 nM, at a SCP2 probe concentration of 1.6 μM, a 4 fold difference in FRET ratio was observed, and hence these concentrations were used for all further experiments pertaining to AEK1.

II. Pilot experiments prior to library screening

Once the optimum concentration of the reagents was determined for the assay, to ensure the reproducibility of the assay, a small scaled multi-well pilot experiment was performed with a known inhibitor for the kinase, DMSO control and a no kinase control. The inhibitor used for Tb11.46.0003 and Tb927.4.5310 was GP29, a *type II* inhibitor that has previously been shown to bind to both the kinases, while the inhibitor used for Tb927.3.2440 (AEK1) was VI-27, the SCP2 probe lacking the Cy5 FRET acceptor.

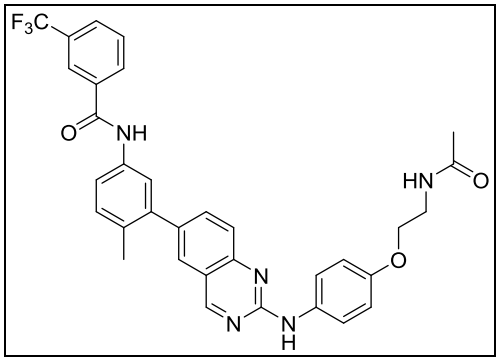

Figure 3. Structure of inhibitor GP29 used in assay against Tb11.46.0003 & Tb927.4.5310.

An assay with 60 wells of reaction mixture containing GP29 (5 μM), SCP2 probe (1.6 μM), and Tb11.46.0003 (160 nM) was set up. These reaction mixtures were to mimic the assay reaction mixtures comprising of inhibitors from the library. The positive control was set up in 24 wells and the negative control was set up in 12 wells. The positive control for the experiment was a reaction mixture comprising of DMSO, SCP2 probe (1.6 μM), and Tb11.46.0003 (160

nM), while the negative control which would give the background FRET ratio was a reaction mixture comprising of DMSO, SCP2 probe (1.6 μM), and assay buffer containing antibody at a final concentration 1 nM (no kinase). Overall, the FRET ratio was consistent in all the wells with the same reaction mixture, indicating that the assay is consistent and robust for probing inhibitor hits of the kinase Tb11.46.0003 at the selected concentrations of the probe SCP2 and kinase (Table A1). The average measured FRET ratio signal of the positive and negative control was higher than that observed in the optimization assay, possibly due to working with smaller volumes of stock protein used in the optimization assays. On comparison of the FRET ratios in wells with reaction mixtures of inhibitor GP29, SCP2 probe and kinase, and negative control, GP29 (5 μM) was 94% bound to the kinase (Table 1). Thus, in the kinase inhibitor library screening, GP29 (5 μM) was used as the negative control to calculate percentage inhibition of the inhibitors and identify inhibitors that are of comparable potency.

Table 1. Summary of FRET ratios of reaction mixture composed of an inhibitor with SCP2 probe and kinase, positive control and negative control against Tb11.46.0003, Tb927.4.5310 & Tb927.3.2440.

	FRET Ratio		
	Tb11.46.0003	Tb927.4.5310	Tb927.3.2440
GP29/VI-27 + SCP2 + Kinase	11.5 ±1.4	7.89 ± 0.043	7.29 ± 0.062
DMSO + SCP2 + Kinase	44.5 ± 0.93	29.0 ± 1.1	43.6 ± 0.79
DMSO + SCP2 + No Kinase	7.45 ± 0.20	7.36 ± 0.13	6.33 ± 0.083

A similar experiment was set up for Tb927.4.5310, but with SCP2 probe concentration of 2.4 μM, and kinase concentration of 240 nM, as determined in the optimization assay. The FRET ratios were consistent in wells with the same reaction mixture (Table A2). While the wells with positive control showed slightly lower FRET signal, than was observed in the optimization

assay, they were still comparable. As compared to the FRET ratio of the reaction mixtures that did not have any kinase, GP29 (5 μM) showed nearly 100% inhibition of Tb927.4.5310 and was thus used as the negative control in the library screening (Table 1).

The inhibitor GP29 does not bind to Tb927.3.2440 (AEK1), thus VI-27 was used as the inhibitor for this kinase. An assay was set up with 48 wells of a reaction mixture containing inhibitor VI-27 (5 μM), SCP2 probe (1.6 μM), and Tb927.3.2440 (120 nM). The positive control was set up in 24 wells and was a reaction mixture of DMSO, SCP2 probe (1.6 μM), and Tb927.3.2440 (120 nM). The negative control was set up in 12 wells, and the FRET ratio was measured for a reaction mixture comprising of DMSO, SCP2 probe (1.6 μM), and antibody with a final concentration of 1 nM diluted in the assay buffer (no kinase). The measured FRET ratios of the wells with no kinase were consistent within themselves, as well as with the data from the optimization assay (Table A3). The positive control wells measured higher FRET ratios as compared to data from the optimization assay but were consistent within the 24 wells. The inhibitor VI-27, at a concentration of 5 μM was nearly 97% bound to AEK1 and was thus used as a negative control in the inhibitor library screening (Table 1).

Inhibitor library screen

After optimization of the assay, a kinase inhibitor library of 429 compounds obtained from Selleck Chem was used to screen for hits against the above mentioned 3 kinases Tb11.46.0003, Tb927.4.5310 & Tb927.3.2440 (AEK1). A reaction was set up in each well in triplicates, comprising of inhibitor from the library (1 μM), SCP2 probe and kinase at optimized concentrations from the above mentioned experiments. GP29 (5 μM) was used for the negative control for Tb11.46.0003 and Tb927.4.5310, whereas VI-27 (5 μM) was used for the negative control for Tb927.3.2440 (AEK1). The positive control for the assay was a reaction mixture of DMSO, SCP2 probe and kinase, while the negative control was a reaction mixture of the

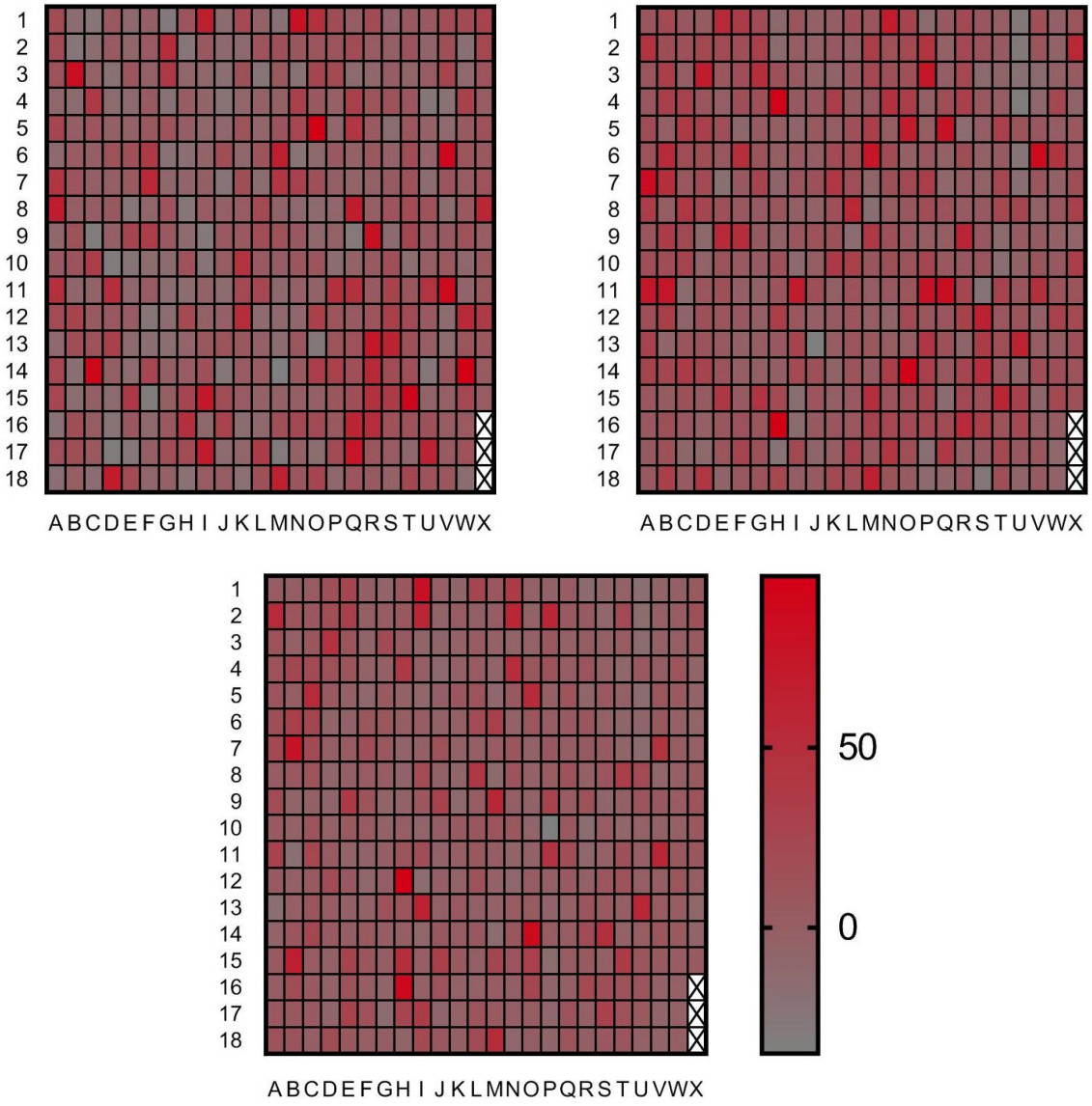

Figure 4. (A) Heatmap showing screening results for Tb11.46.0003. (B) Heatmap showing screening results for Tb927.4.5310. (C) Heatmap showing screening results for Tb927.3.2440. Color gradient for % inhibition shown alongside.

inhibitor (GP29/VI-27), SCP2 probe and kinase. The average of the FRET ratio of both the controls in each plate was used to calculate percentage inhibition of each inhibitor. The positive control yielded nearly 20% higher FRET ratio for Tb11.46.003 and Tb927.4.5310 as compared to that observed in the optimization assays, though they were consistent between the various assay plates. The negative control from the library screening assay was consistent with that as observed in the optimization assays. The positive control and negative control for AEK1,

although consistent across the different plates in the assay in the screening, yielded nearly 50% higher FRET ratios as compared to the FRET ratios of the positive and negative control as observed in the optimization assays. The screening results for the three kinases are shown in a heatmap format (Figure 4). Potent inhibitors (hits) from the screen are shown in bright red, while the inhibitors that were not as potent are in gray. Hits from the screen were consistent in all three data sets, with low percentage error, which indicates that this TR-FRET assay is robust and reproducible. Inhibitors that were not a potent hit in the screen, yielded high FRET ratios as compared to the average of the positive control, attributing to a high percentage error and negative percentage inhibition as seen in the heat map.

Inhibitor hits for Tb11.46.0003 & Tb927.4.5310

The most potent inhibitors that were recognized from the screening competed away the substrate with more than 85% inhibition and are listed below (Table 2, 3). Six of the hits (RAF-265, SC1 (Pluripotin), AT9283, KW-2449, GZD824 and G-749) were inhibitors for both the kinases. Three of these common hits - RAF-265, SC1 (Pluripotin) and GZD824 are *type II* inhibitors, while, rebastinib, sorafenib and regorafenib are *type II* inhibitors, that were a hit in the library screening against Tb11.46.0003, but not Tb927.4.5310. Two inhibitor hits from the screening against Tb927.4.5310 - R406 and R406 (free base) that only differ in the counter salt ion, indicates that the assay is consistent in identifying hits.

To confirm hits from this screening, dose-response curves for 4 *type II* inhibitors- RAF-265, SC1 (Pluripotin), GZD824, and Rebastinib against both the kinases were generated (Figure 5). The inhibitors were diluted 2-fold down from a concentration of 10 μM to 19.5 nM. A 20 μL reaction was set up in each well with the same concentration of SCP2 probe and kinase as well as positive and negative control as in the inhibitor library screening experiment.

Table 2. List of hits from kinase inhibitor library screening of Tb11.46.0003.

	Inhibitor	% Inhibition
1	AZD5363	86 ± 1
2	AT9283	85 ± 4
3	DCC-2036 (Rebastinib)	79 ± 1
4	G-749	78 ± 9
5	SC1 (Pluripotin)	77 ± 2
6	SGI-7079	76 ± 5
7	AZD5438	72 ± 6
8	URMC-099	70 ± 2
9	RAF265 (CHIR-265)	68 ± 3
10	TPCA-1	64 ± 5
11	VE-822	62 ± 9
12	GNE-9605	62 ± 7
13	Sorafenib Tosylate	58 ± 10
14	Bosutinib (SKI-606)	58 ± 20
15	SU11274	57 ± 7
16	GZD824	54 ± 5
17	Regorafenib	56 ± 10
18	TAK-901	55 ± 10
19	KW-2449	54 ± 4
20	IKK-16	51 ± 8

Table 3. List of hits from kinase inhibitor library screening of Tb927.4.5310.

	Inhibitor	% Inhibition
1	R406 (free base)	92 ± 2
2	R406	89 ± 3
3	Crizotinib (PF-02341066)	87 ± 2
4	SC1 (Pluripotin)	80 ± 4
5	BMS-536924	79 ± 1
6	CYT387	78 ± 3
7	FRAX597	73 ± 7
8	CYC116	72 ± 4
9	GZD824	69 ± 6
10	TDZD-8	67 ± 3
11	Dabrafenib (GSK2118436)	67 ± 2
12	JNJ-7706621	67 ± 4
13	AT9283	63 ± 8
14	RAF265 (CHIR-265)	63 ± 8
15	GSK2334470	62 ± 8
16	Piceatannol	60 ± 5
17	Quercetin	58 ± 7
18	KW-2449	57 ± 4
19	PF-431396	54 ± 5
20	G-749	51 ± 2

As seen in the individual dose response curves, the four analyzed inhibitors RAF-265, Rebastinib, SC1 (Pluripotin) and GZD824 showed similar percentage inhibition in both the primary inhibitor library screening assay, as well as inhibitor titration assay (Figure 5). The

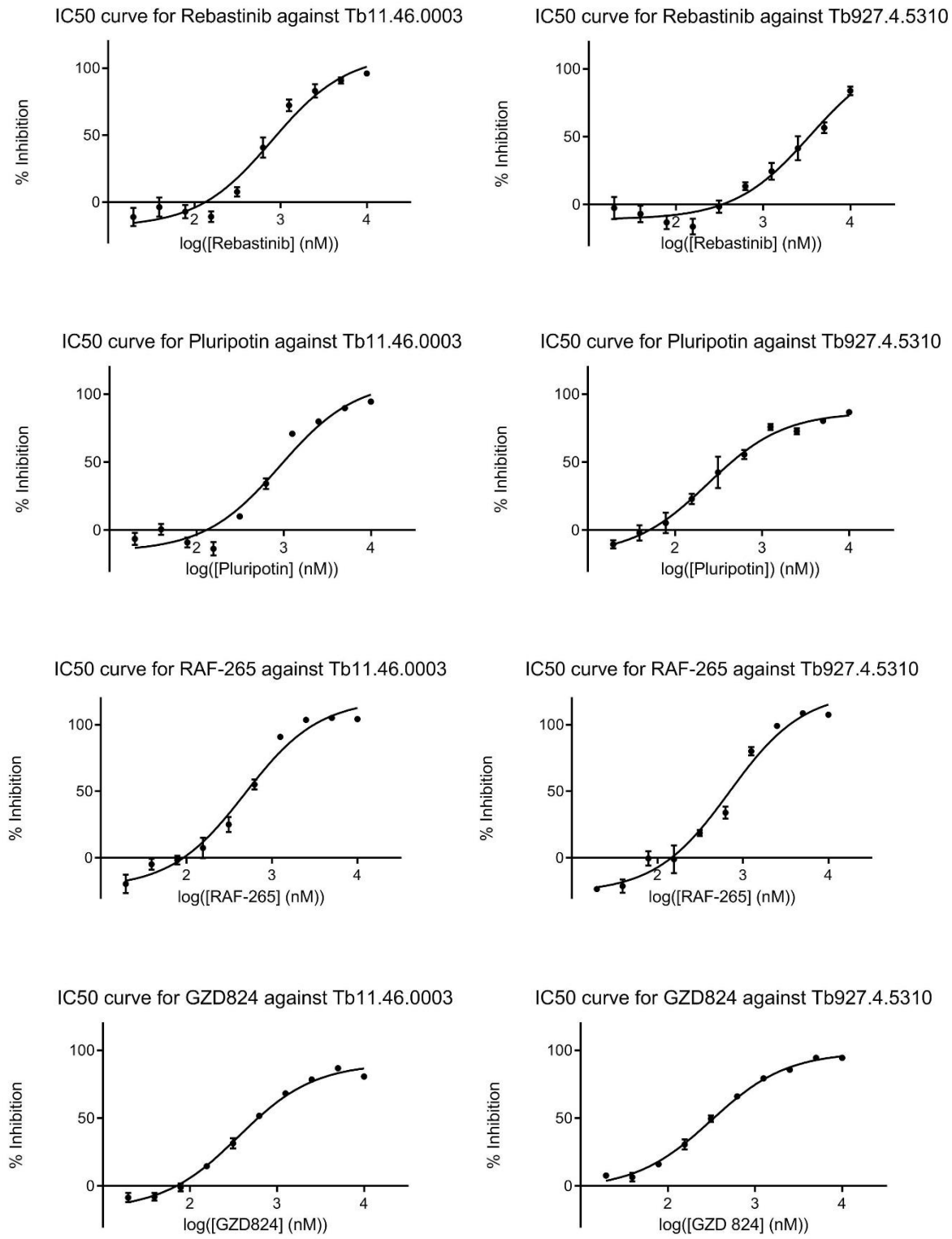

Figure 5. Dose-response curves for Rebastinib, SC1 (Pluripotin), RAF-265 & GZD824 against Tb11.46.0003 & Tb927.4.5310.

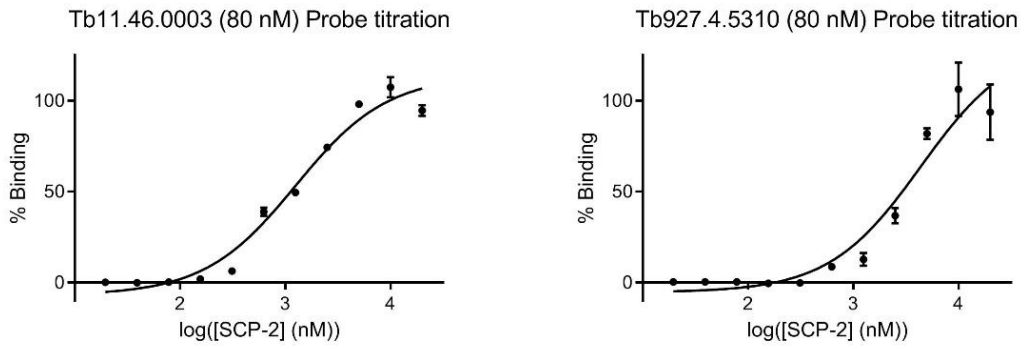

Figure 6. Binding curves for SCP2 probe against Tb11.46.0003 (80 nM) & Tb927.4.5310 (80 nM).

dose-response curves reached a plateau at highest concentrations of the inhibitor and were used to calculate the half maximal inhibitory concentration (IC_{50}) using one site log IC_{50} fitting. Rebastinib, which is a hit for Tb11.46.0003, but not for Tb927.4.5310, had an IC_{50} of 820 ± 120 nM for Tb11.46.0003, and a 5-fold higher IC_{50} of 3960 ± 1000 nM for Tb927.4.5310, indicating the sensitivity of the assay to identify hits for a target kinase.

To find the inhibition constant K_i of the 4 inhibitors, the dissociation constant K_d for the kinases and SCP2 probe was calculated. The SCP2 probe was diluted 2-fold down from a concentration of 20 μM to 19.5 nM. A 20 μL reaction with DMSO, SCP2 probe and kinase at 80 nM was set

Table 4. Summary of IC_{50} and K_i values for the 4 inhibitors RAF-265, Pluripotin, Rebastinib and GZD824 against Tb11.46.0003 & Tb927.4.5310.

	Tb 11.46.0003		Tb 927.4.5310	
	IC_{50} (nM)	K_i (nM)	IC_{50} (nM)	K_i (nM)
RAF-265	482 ± 58	212 ± 28	691 ± 81	452 ± 140
Pluripotin	907 ± 63	400 ± 34	247 ± 61	162 ± 62
Rebastinib	820 ± 120	361 ± 56	3960 ± 1000	2590 ± 1000
GZD824	371 ± 56	164 ± 26	314 ± 14	205.3 ± 60

up. The K_d values were determined to be 1260 ± 58 nM for Tb11.46.0003, and 4540 ± 1100 nM for Tb927.4.5310 (Figure 6). The K_i values were then calculated using the Cheng-Prusoff equation ($K_i = IC_{50} / 1 + [S]/K_d$). Based on these values, GZD824 had similar potency for both these kinases, whereas RAF-265 was more potent for Tb11.46.0003 and Pluripotin for Tb927.4.5310 with K_i values of around 200 nM (Table 4).

The data from the library screen as well as individual dose-response curves validates earlier chemical proteomics and BODIPY assay experiments done in our lab. Through those experiments, it was established that kinases Tb11.46.0003 and Tb927.4.5310 are two essential kinases for *T. brucei* that bind selectively to a general *type II* inhibitor GP29 containing a trifluoromethyl moiety. The TR-FRET assay results also indicate that the two kinases bind to GP29, and further establish that 3 inhibitors that contain the trifluoromethyl moiety RAF-265, GZD824 and pluripotin (SC1) are also potent for both the kinases.

Inhibitor hits for Tb927.3.2440 (AEK1)

AEK1 did not have as many potent hits as Tb927.4.5310 or Tb11.36.0003, though the most potent inhibitor, Hesperadin showed above 95% inhibition. The hits from the screen for AEK1 are listed below (Table 5). Two inhibitors, R406 (with and without free base) and PF-431396 were found to be potent for both Tb927.4.5310 as well as AEK1. Two other inhibitors, TAK-901 and SGO-7079 were common hits for Tb11.46.0003 and AEK1, while AT9283 and KW2449 were found to be potent for all three kinases, neither of which are identified *type II* inhibitors. Amongst the 17 identified hits from the screen for AEK1, only three of the inhibitors were identified as *type II* inhibitors, Axitinib, Foretinib and PF-431396. These hits were not confirmed individually but based on the data from the library screening against Tb11.46.0003 and Tb927.4.5310 that confirmed the consistency of hits identified in the screening assay, it can be concluded that these inhibitors were also hits for Tb927.3.2440 (AEK1).

Table 5. List of hits from kinase inhibitor screening of Tb927.3.2440 (AEK1).

	Inhibitor	% Inhibition
1	Hesperadin	97 ± 4
2	R406 (free base)	87 ± 5
3	R406	85 ± 7
4	TAK-901	80 ± 7
5	PF-477736	77 ± 5
6	Cediranib (AZD2171)	63 ± 6
7	PF-3758309	62 ± 8
8	AZD1480	57 ± 10
9	SGI-7079	56 ± 2
10	AZ 960	56 ± 6
11	Foretinib (GSK1363089)	56 ± 9
12	AMG-900	56 ± 9
13	PF-431396	55 ± 4
14	BX-912	53 ± 10
15	Axitinib	52 ± 20
16	AT9283	52 ± 10
17	KW-2449	52 ± 10

Kinase inhibitors have been of prime interest in pharmaceuticals. Some of the hits from the inhibitor library screening against the three kinases that could serve as potential drug targets for HAT, are FDA-approved drugs, and a few others are in clinical trials. While further biochemical characterization of these inhibitors is required to establish their therapeutic potential for HAT, they serve as leads for further drug optimization.

Conclusion

The TR-FRET based assay described in this thesis uses a probe called SCP2 that was optimized to bind to multiple kinases in their active site to emit a FRET signal with an Eu labeled antibody. The SCP2 probe binds to three essential kinases, namely Tb11.46.0003, Tb927.4.5310 and Tb927.3.2440 (AEK1) of the trypanosome kinome that were earlier established to be essential for the infecting parasite of HAT and could be potential drug targets. This assay method is hence used to identify ATP-competitive inhibitors that bind to these kinases by competing against the SCP2 probe, attenuating the FRET signal. Using this technique, hits were identified from a library of 429 kinase inhibitors for each of the three kinases, that were further confirmed by individual inhibitor dose response curves for two of the kinases, to determine their inhibition constants. The major focus of the study was on *type II* inhibitors, a class of inhibitors that have shown higher specificity for their targets, owing to their interaction with the hydrophobic pocket beside the active core. Although this assay was used to probe binding of small molecules to kinases of the trypanosome kinome, it can be further developed into an HTS assay method for other kinomes too. In summary, a novel TR-FRET based assay that had been developed, was applied to the *Trypanosoma brucei* kinome system for inhibitor hit screening and their validation, establishing the robustness, reproducibility and sensitivity of the assay.

References

1. Trypanosomiasis, human African (sleeping sickness). http://www.who.int/news-room/fact-sheets/detail/trypanosomiasis-human-african-(sleeping-sickness) (accessed Nov 2, 2018).
2. Alderton, S.; Macleod, E. T.; Anderson, N. E.; Palmer, G.; Machila, N.; Simuunza, M.; Welburn, S. C.; Atkinson, P. M. *PLOS Neglected Tropical Diseases* **2018**, *12*(2).
3. Kennedy, GE. P.; Lancet, 375 (**2013**), pp. 148-159;
4. Rijo-Ferreira, F.; Carvalho, T.; Afonso, C.; Sanches-Vaz, M.; Costa, R. M.; Figueiredo, L. M.; Takahashi, J. S. *Nature Communications* **2018**, *9*(1).
5. Stich, A. *Bmj* **2002**, *325*(7357), 203–206.
6. Parasites. https://www.cdc.gov/parasites/sleepingsickness/ (accessed Nov 25, 2018).
7. African Trypanosomiasis Clinical Presentation. https://emedicine.medscape.com/article/228613-clinical (accessed Nov 25, 2018).
8. Maclean, L.; Reiber, H.; Kennedy, P. G. E.; Sternberg, J. M. *PLoS Neglected Tropical Diseases* **2012**, *6*(10).
9. Kennedy, P. G. E. *Annals of Neurology* **2008**, *64*(2), 116–126.
10. Symptoms, diagnosis and treatment. http://www.who.int/trypanosomiasis_african/disease/diagnosis/en/ (accessed Nov 25, 2018).
11. Kennedy, P. G. *The Lancet Neurology* **2013**, *12*(2), 186–194.
12. Phosphorylation, Ubiquitylation and Drug Discovery. http://www.kinase-screen.mrc.ac.uk/phosphorylation-ubiquitylation-drug-discovery (accessed Nov 25, 2018).
13. Roskoski, R. *Pharmacological Research* **2016**, *103*, 26–48.
14. Noble, M. E. M. *Science* **2004**, *303*(5665), 1800–1805.

15. Cohen, P.; Alessi, D. R.; *ACS Chem. Biol.*, **2013**, *8* (1), pp 96–104.
16. Jones, N. G.; Thomas, E. B.; Brown, E.; Dickens, N. J.; Hammarton, T. C.; Mottram, J. C. *PLoS Pathogens* **2014**, *10*(1).
17. Jensen, B. C.; Booster, N.; Vidadala, R. S. R.; Maly, D. J.; Parsons, M. *International Journal for Parasitology* **2016**, *46*(8), 479–483.
18. Hughes, J.; Rees, S.; Kalindjian, S.; Philpott, K. *British Journal of Pharmacology* **2011**, *162*(6), 1239–1249.
19. A powerful tool for drug discovery. https://www.europeanpharmaceuticalreview.com/article/3090/a-powerful-tool-for-drug-discovery/ (accessed Nov 25, 2018).
20. Du, Y.; Fu, R. W.; Lou, B.; Zhao, J.; Qui, M.; Khuri, F. R.; Fu, H. *ASSAY and Drug Development Technologies* **2013**, *11*(6), 367–381.
21. LANCE Eu-anti-6xHis antibody-AD0205-AD0110-AD0111. http://www.perkinelmer.com/product/lance-eu-anti-6xhis-antibody-10-ug-ad0205 (accessed Nov 28, 2018).
22. Studier, F. W. *Protein Expression and Purification* **2005**, *41*(1), 207–234.
23. Hari, S. B.; Perera, B. G. K.; Ranjitkar, P.; Seeliger, M. A.; Maly, D. J. *ACS Chemical Biology* **2013**, *8*(12), 2734–2743.

Appendix

Table A1. FRET ratio of multi-well reaction mixtures comprising of inhibitor GP29, positive control and negative control for Tb11.46.0003 (concentrations mentioned in brackets).

GP29 (5 µM) + SCP 2 (1.6 µM) + Tb11.46.0003 (160 nM)	9.99	11.0	9.04	9.41	9.21	9.37	94.8	9.16	9.61	9.29	13.9	8.77
	8.27	9.02	10.1	10.1	10.2	9.98	17.8	9.88	10.1	9.58	13.1	9.29
	8.44	8.83	9.27	9.08	9.34	9.25	18.3	9.64	9.12	8.86	12.4	8.73
	8.30	8.76	9.03	8.94	9.07	9.01	17.7	9.50	8.90	10.2	12.1	8.89
	8.21	8.46	8.94	8.67	8.80	9.13	15.9	8.93	9.37	9.22	11.9	11.4
DMSO + SCP 2 (1.6 µM) + Tb11.46.0003 (160 nM)	46.7	48.0	50.1	47.0	50.7	47.2	40.3	43.3	44.5	42.5	33.5	40.4
	44.4	45.8	48.2	49.6	46.2	41.5	46.2	44.2	49.7	44.8	34.9	38.2
DMSO + SCP 2 (1.6 µM) + No kinase	6.85	6.87	6.96	7.27	7.24	7.27	7.46	7.25	9.32	7.65	6.75	8.06

Table A2. FRET ratio of multi-well reaction mixtures comprising of inhibitor GP29, positive control and negative control for Tb927.4.5310 (concentrations mentioned in brackets).

GP29 (5 µM) + SCP 2 (2.4 µM) + Tb927.4.5310 (240 nM)	8.77	8.65	8.89	7.71	7.40	7.78	7.93	8.32	8.02	7.73	8.01	8.09
	8.00	7.59	7.75	7.94	7.84	8.01	7.89	8.04	8.48	7.71	7.91	7.56
	7.55	7.58	7.45	7.63	8.13	7.29	7.65	7.76	8.06	7.91	8.12	7.80
	7.39	7.61	7.95	7.87	7.89	7.54	7.61	7.66	7.56	8.18	8.19	8.26
	8.22	7.46	8.40	8.07	7.93	7.82	7.74	7.62	7.68	8.02	7.79	7.95
DMSO + SCP 2 (2.4 µM) + Tb927.4.5310 (240 nM)	44.9	27.7	31.8	32.1	28.2	28.5	26.6	30.2	23.8	31.8	30.6	24.4
	41.6	28.5	27.5	27.3	24.6	28.4	29.3	29.7	25.2	22.8	28.8	21.0
DMSO + SCP 2 (2.4 µM) + No kinase	8.44	7.34	7.02	7.27	7.17	6.96	7.34	7.18	7.32	7.71	7.73	6.80

Table A3. FRET ratio of multi-well reaction mixtures comprising of inhibitor VI-27, positive control and negative control for Tb927.3.2440/AEK1 (concentrations mentioned in brackets).

VI-27 (5 µM) + SCP 2 (1.6 µM) + AEK1 (120 nM)	7.49	7.29	7.44	7.36	7.35	6.71	7.49	7.34	7.60	7.22	7.48	6.19
	7.30	7.66	7.11	7.40	7.23	8.04	7.78	7.74	7.90	7.62	7.71	6.37
	7.33	7.35	6.79	6.77	6.81	7.14	7.06	7.12	7.15	7.07	6.61	6.21
	7.35	7.66	7.39	7.36	7.77	7.50	7.70	7.79	7.50	7.57	7.66	6.58
DMSO + SCP 2 (1.6 µM) + AEK1 (120 nM)	46.1	42.9	51.7	50.4	45.8	46.1	47.7	44.6	40.7	43.1	42.6	38.9
	37.8	35.9	40.5	45.7	44.0	44.2	45.3	46.7	44.2	43.5	40.5	37.5
DMSO + SCP 2 (1.6 µM) + No kinase	5.81	6.23	6.21	6.16	6.65	6.31	6.67	6.69	6.57	6.29	6.45	5.93

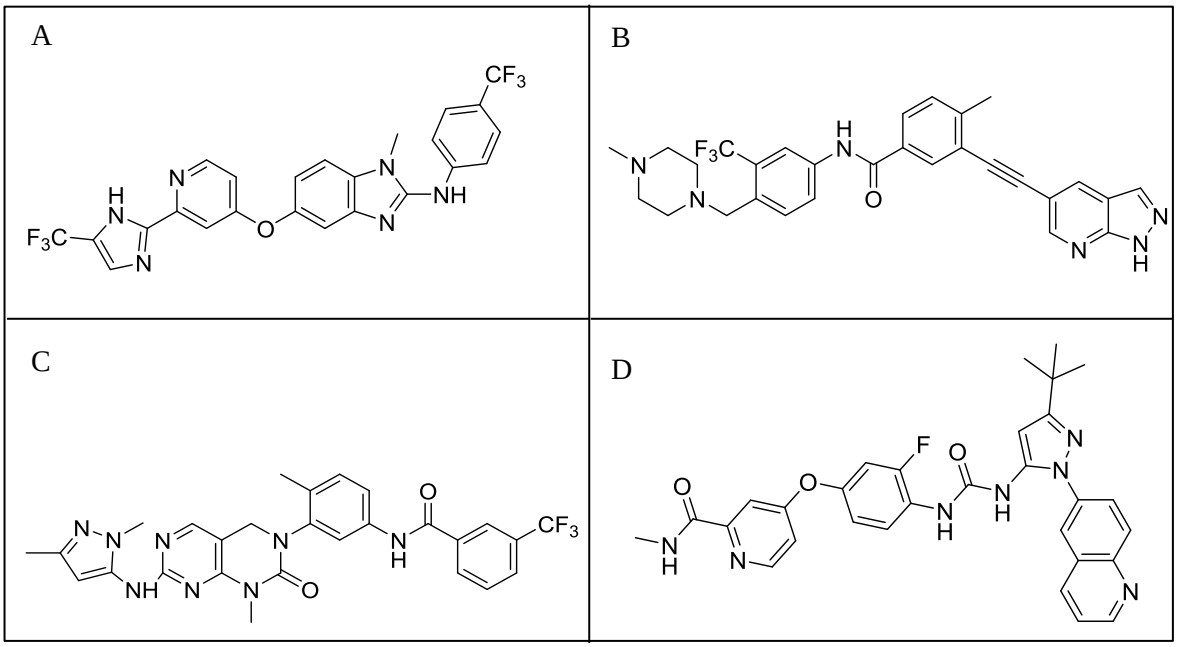

Figure A1. (A) Structure of RAF-265. (B) Structure of GZD824. (C) Structure of SC1 (Pluripotin). (D) Structure of Rebastinib.